CrossMark

ORIGINAL PAPER

Fabrication of a new gel polymer electrolyte containing core–shell silica–polyelectrolyte nanoparticles via activators regenerated by electron transfer atom transfer radical polymerization (ARGET-ATRP) for high-performance lithium–sulfur batteries

Mohammad Reza Sovizi[1] · Ali Reza Madram[1]

Abstract Presented herein is the fabrication of a new gel polymer electrolyte (GPE) containing core–shell nanoparticles for lithium–sulfur (Li–S) batteries. This work is to overcome drawbacks of poly (vinylidenefluoride) (PVDF)-based GPEs while simultaneously maintaining their beneficial electrochemical properties such as high ionic conductivity at ambient temperature and excellent chemical stability. Core–shell silica nanoparticles with silica as core and poly (vinylbenzenesulfonate) as shell was synthesized via activators regenerated by electron transfer atom transfer radical polymerization and incorporated into PVDF. The obtained composite displays ionic conductivity as high as 1.1 mS cm^{-1} at room temperature. Electrochemical experiments show that the new GPE acts as an effective electrolyte for high-performance lithium–sulfur batteries.

Keywords Gel polymer electrolyte · Lithium–sulfur batteries · Core–shell silica

Introduction

The lithium-ion rechargeable batteries have been widely used in the portable electronic devices such as laptops, cameras and cell phones due to their high specific energy and power density (Wang et al. 2002; Ugur et al. 2014). However, the energy and power densities of rechargeable lithium batteries require significant improvement to power electric vehicles. Thus far, the lower specific capacities of cathode materials (150 mAhg^{-1} for layered oxides and 170 mAhg^{-1} for LiFePO$_4$) (Oriňáková et al. 2013) compared to those of the anode (370 mAhg^{-1} for graphite and 4200 mAhg^{-1} for Si) have been a limiting factor to the energy density of batteries. It is highly desirable to develop and optimize high capacity cathode materials for rechargeable lithium batteries (Whittingham 2004; Kim et al. 2011; Kumar et al. 2012; Mondal et al. 2014; Thirunakaran et al. 2014).

Sulfur has a theoretical specific capacity of 1672 mAhg^{-1} about 5 times higher than those of traditional cathode materials based on transition metal oxides or phosphates which make lithium–sulfur (Li/S) redox couple a promising candidate for high energy density batteries (Ji et al. 2009; Ji et al. 2011a, b; Li et al. 2013; Wang et al. 2014). However, it has been difficult to develop a practical Li/S battery due to the low electrical conductivity of sulfur and dissolution of polysulfides into liquid electrolytes. Furthermore, conventional liquid electrolytes used in Li/S batteries are volatile and flammable, leading to a number of safety concerns and severely limiting their overall application (Zhan et al. 2008; Hassoun and Scrosati 2010; Kim et al. 2012; Yeon et al. 2013; Zhang 2013).

For the last two decades, consistent research has been focused on developing more reliable electrolytes for Li/S batteries. One of the most viable alternatives to liquid electrolytes is a gel polymer electrolyte (GPE). Among all GPEs, poly (vinylidenefluoride) (PVDF) is one of the most studied ones because of its good electrochemical stability, plasticity and liquid electrolyte uptake (Reddy et al. 2007; Li et al. 2008). However, most of the Li/S batteries comprised of GPEs suffer from performance fading after a few cycles due to the poor liquid electrolyte upholding of the electrolyte membrane (Zhang et al. 2011). A wide variety of approaches have been studied to enhance the

✉ Mohammad Reza Sovizi
mrsovizi@mut.ac.ir

[1] Department of Chemistry, Malek Ashtar University of Technology, P.O.Box 16765-3454, Tehran, Iran

performance of PVDF based GPEs in these batteries. Fillers such as SiO_2, Al_2O_3, and TiO_2 can improve mechanical and electrical properties of polymer electrolytes (He et al. 2005; Yang et al. 2006; Das et al. 2011; Ji et al. 2011a, b; Lee et al. 2012). Silica nanoparticles can adsorb polysulphide anions through interaction with positively charged Si–O group on the nanoparticle surface (Ji et al. 2011a, b). Along with that, surface modification of nanoparticles using a proper polyelectrolyte can also promote ionic conductivity of polymer electrolyte (Lee et al. 2012; Zhang et al. 2014). There are various methods for surface modification of nanoparticles. Among them, methods based on controlled radical polymerizations and specifically Activators Regenerated by electron transfer atom transfer radical polymerization (ARGET-ATRP) are unique due to their relatively simple, control over molecular weight, low poly disparities, and molecular architecture (Ohno et al. 2005; Matyjaszewski 2012).

In this study, core–shell silica nanoparticles with poly (vinyl benzene sulfonate) as shell was synthesized, and incorporated into PVDF to form a GPE. This study was prompted by the belief that addition of small amounts of a proper nanoparticle with proper surface modification can promote the morphology of polymer membrane and improve the performance of lithium–sulfur batteries. The obtained results confirm the improved performance of this polymer electrolyte in lithium–sulfur batteries.

Experimental

Silica nanoparticles synthesis

Silica nanoparticles were made using a sol–gel process based on the Stöber method (Stöber et al. 1968). A typical procedure to make an 80 nm silica particle was as follows: at room temperature, 4 ml of tetraethylortho-silicate (TEOS) (Sigma-Aldrich, USA) was added to 50 ml of ethanol (Merck, Germany). The pH was adjusted using 8 ml of ammonium hydroxide (Merck, Germany) solution (25 wt%). The condensation of TEOS was carried out for 6 h and the particles size was monitored using dynamic light scattering (DLS). At the end of the reaction, the silica dispersion was centrifuged at 14,000 rpm and washed with ethanol, this process being repeated four times. The resultant silica nanoparticles were dried in an oven for 48 h at 75 °C.

### Surface modification of silica nanoparticle

To have core–shell silica nanoparticles, surface-initiated ARGET-ATRP method is used to polymerize sodium 4-vinylbenzenesulfonate (NaStaS) on the surface of silica nanoparticles. Since the silica particles have hydroxyl functional groups on their surface, it is possible to attach the bromide initiator to the surface (Nyström et al. 2005). That being the case, the initiator first attached to the silica particles in two steps: first (3-aminopropyl) trimethoxy silane (APTES) (Merck, Germany) is attached covalently to the surface, then bromoisobutyryl bromide (BiBB) (Merck, Germany) as ATRP initiator is attached to the amine group of APTES. The whole procedure is as follows: 3.2 g of silica nanoparticles are dispersed in 300 ml ethanol contains 10 ml ammonium hydroxide solution (25%), and then 6 ml of 3-aminopropyltriethoxy silane (APTES) is added to the solution and stirred for 24 h at 75 °C. The particles are centrifuged and washed with ethanol six times and dried in oven overnight. The initiator is attached to the amine group of APTES as the following procedure: 0.5 g of APTES is dispersed in 100 ml dichloromethane (DCM) (Merck, Germany), then 1.392 ml of triethyle amine (Merck, Germany), 1.024 ml of BiBB (Merck, Germany), and 0.0122 g of dimethyl amino pyridine (DMAP) (Merck, Germany) are added to the suspension and stirred for 12 h. The resulting nanoparticles are washed and centrifuged four times with DCM and finally dried under vacuum at 60 °C for 24 h. Afterwards, to have PNaStS core–shell layer on silica nanoparticles (Iddon et al. 2004; Min et al. 2007), 0.3 g silica modified with initiator and 1.78 g of sodium 4-vinylbenzenesulfonate (Merck, Germany) is dispersed in 50 vol.% solution of methanol (Merck, Germany) and water. In another vial, 1.75 mg of $CuBr_2$ (Merck, Germany) as catalyst, 3.2 µl of 1, 1, 4, 7, 10, 10-hexamethyltri-ethylenetetramine (HMTETA) (Merck, Germany) as ligand, and 1.38 mg ascorbic acid (Vitamin C) (Merck, Germany) as reducing agent to continuously reduce $CuBr_2$ to CuBr during reaction polymerization reaction was carried on for 6 h in 20 °C. Before performing the polymerization reaction, the vial atmosphere was purged with nitrogen. At the end, the reaction was stopped by exposure to air. The nanoparticles were washed and centrifuged four times with water and then dried for 48 h in vacuum oven.

After surface modification with polyelectrolyte, the sodium ions in the polymer should be replaced with lithium ions. To this aim, the core–shell silica nanoparticles were dispersed in dimethyl sulfoxide. Lithium hydroxide crystals were dissolved in the solution to replace Li^+ ions with Na^+ under nitrogen atmosphere at 80 °C for 12 h. The resulting nanoparticles were dispersed in PVDF-DMF-Acetone solution using ball-mill. After dispersion of nanoparticles, a uniform film was formed through reverse phase separation and then dried at 75 °C in vacuum oven.

Preparation of composite gel polymer electrolytes

The slurry for preparation of membrane was prepared by polyvinylidene fluoride (PVDF; Kynar, HSV900, USA)
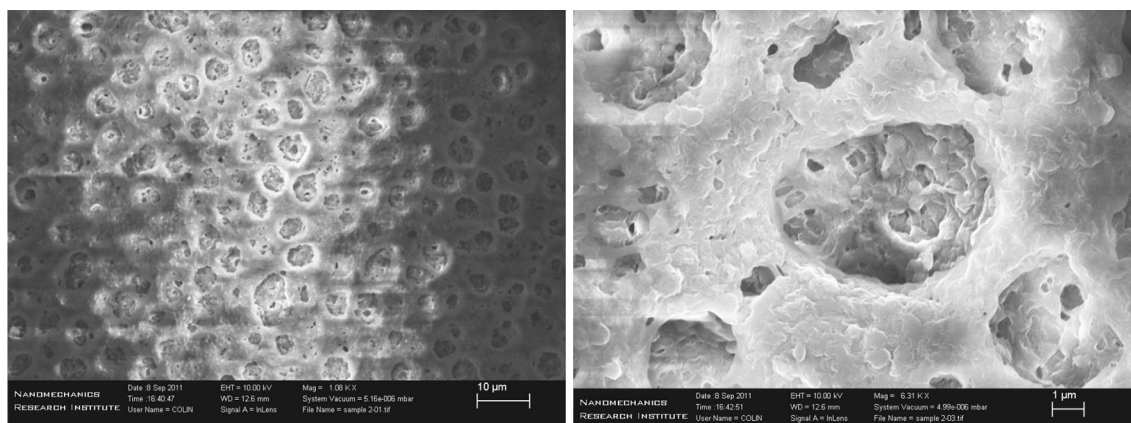
Fig. 1 Scanning Electron microscopy (SEM) of S-KB/PVDF/AB (70:20:10 wt%) cathod, **a** 1 kx, and **b** 6 kx

and core-shell silica nanoparticles with dimethylformamide (DMF) and acetone (Merck, Germany) as solvents in a ball-mill. The porous films with 500 μm thickness were made by the inverse phase separation method after immersion of the membrane in water. Afterwards, the composite membrane was dried at 75 °C in vacuum oven for 24 h. The gel polymer electrolyte was formed after soaking the porous membrane in a liquid electrolyte, consisting of a 1 M lithium bistrifluoromethanesulfonamide (LiTFSI) (99.95%, Sigma- Aldrich, USA) dissolved in in 1:1 v/v 1, 2-dimethoxyethane (DME) (Sigma- Aldrich, USA) and 1, 3-dioxolane (DOL) (Sigma- Aldrich, USA) for 30 min.

Electrode preparation and cell assembly

Ketjen black (KB, Akzo Nobel, EC-600 JD) a porous carbon with high specific surface area of 1400 m^2 g^{-1} was used as a matrix to prepare Sulfur-KB composite cathode material. Sulfur (100-mesh particle size powder, Sigma-Aldrich) and KB powder in a weight ratio of 10:4 was used to prepare the S–KB composite by employing a solution processing method (Ryu et al. 2013). First, sulfur powder was dissolved in dimethyl sulfoxide (DMSO) at 120 °C by vigorously stirring for 2 h. Then, the KB powder was added to the solution and dispersed by stirring for 4 h and while being stirred it was cooling to room temperature overnight. Within this process, the dissolved sulfur molecules were recrystallized in the highly porous structure of the KB, resulting in a sulfur–carbon composite. Finally, the composite powder was washed with ethanol and milli-Q water several times for removal residual DMSO and then dried in a vacuum at 100 °C to evaporate ethanol and water. The composite showed 51.1 wt% sulfur from the result of TGA (TA instruments, Q-600); it is lower than the added sulfur powder content 71.4 wt%. Apparently, some amount of sulfur (20.3 wt%) did not recrystallize in the

composite powder after being dissolved in DMSO solvent and was washed away by ethanol at the dissolving state.

The S-KB cathode electrode was prepared by mixing of 70, 20, and 10 wt% for S-KB composite, acetylene black (AB, MTI, 99.5% purity) as conductive agent and polyvinylidene fluoride (PVDF, Kynar, HSV900) as a binder with NMP (Sigma-Aldrich, ≥99.5% purity) as a dispersant, respectively. The obtained slurry was then applied to an Al foil current collector and was dried in a drying oven at 70 °C for 12 h. Figure 1 shows morphology of the prepared cathode and homogeneity of compounds.

The electrochemical properties were obtained using coin cells with a lithium metal anode, a sulfur–carbon cathode and the gel polymer electrolyte as electrolyte. AC impedance spectroscopy was performed on the coin cells using a potentiostat (VMP3, BioLogic) in the frequency range of 0.1 Hz to 1 MHz. An Arbin BT2000 battery testing system in galvanostatic mode was used to examine the cycling performance of the cells at room temperature and 1.5 to 3.0 V.

Characterization

For investigation morphology of the nanoparticles and electrolytes, field emission scanning electron microscopy (FE-SEM) (Ultra, Zeiss) was used. The samples were gold-sputtered prior to SEM. Transmission electron microscopy (TEM) (Philips CM20) was used at an accelerating voltage of 100 kV. About 20 μl of nanoparticle suspension was placed on a holey carbon grid (400-mesh) for 2 min. Then any remaining solution was drawn off the edge of the grid with tissue paper and the grid was washed with 20 μl of deionized water. The prepared grids were air-dried for 1 h before starting the TEM measurements. The particle size distribution of nanoparticles was measured by a Zetasizer Nano ZS (Malvern Instruments, Worcestershire, UK) through Dynamic Light Scattering (DLS) method. The

Fig. 2 Intensity based size distribution of silica nanoparticles obtained by dynamic light scattering (DLS) at 25 °C (**a**), transmission electron microscopy (TEM) at 180 kx (**b**), scanning electron microscopy (SEM) at 100 kx (**c**)
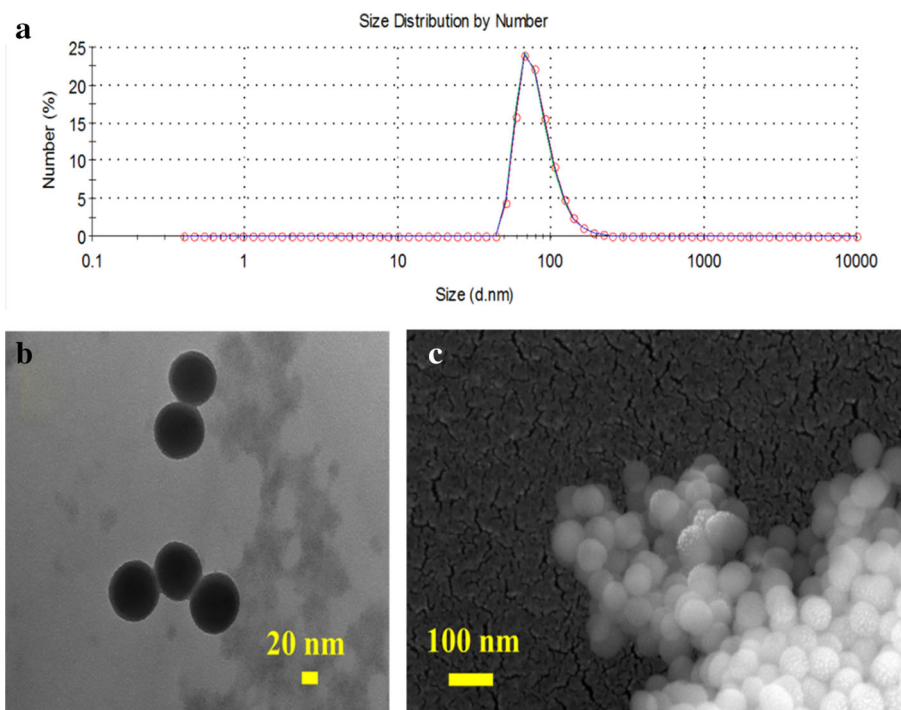
Fig. 3 Scanning electron microscopy (SEM) of silica nanoparticles after surface-initiated ARGET-ATRP with PNaStS, **a** 20 kx, and **b** 60 kx
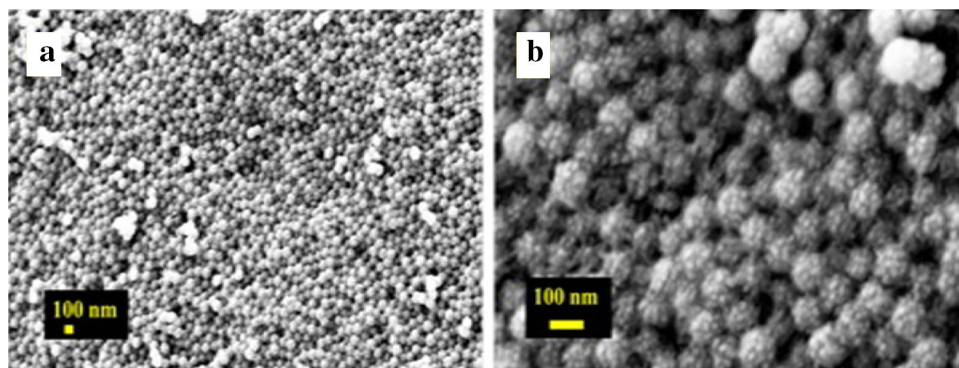
parameters such as viscosity and refractive index were set for each measurement at 25 °C.

Change in surface chemistry of nanoparticles was confirmed with Fourier transform infrared spectroscopy (FTIR; Bruker Tensor 27). A thermo gravimetry differential analysis (TGA) apparatus (TA instruments, Q-600) is used to determine organic content on the surface on nanoparticles in a temperature ramp mode and a heating rate of 10 °C min^{-1} up to 800 °C.

Results and discussion

The intensity-based size distribution of the silica nanoparticles is obtained using DLS is shown in Fig. 2a. The DLS result exhibits a narrow distribution of particles with a z-average of 80 nm. The results of three

measurements are superimposed on each other. Transmission electron microscopy (TEM) image, Fig. 2b, also shows uniform size distribution of nanoparticles. The SEM result after surface modification with amine group in Fig. 2c also shows no change in size of nanoparticles after modification with APTES.

The morphology of nanoparticles after surface-initiated ARGET-ATRP, Fig. 3, shows an increase in diameter of nanoparticles up to 100 nm. Besides the size, the presence of poly electrolyte on the surface has changed the surface morphology of the nanoparticles.

To confirm the presence of modification on silica nanoparticles FTIR and TGA analysis was performed and the resulting spectrums are shown in Figs. 4 and 5, respectively.

In the FTIR spectrum, the Si–O peaks at 800 and 1100 cm^{-1}, Si–OH at 950 cm^{-1}, the broad OH peak in

Fig. 4 FTIR spectrum for silica (*top*), silica modified with APTES (*middle*), and silica modified with initiator (*bottom*)
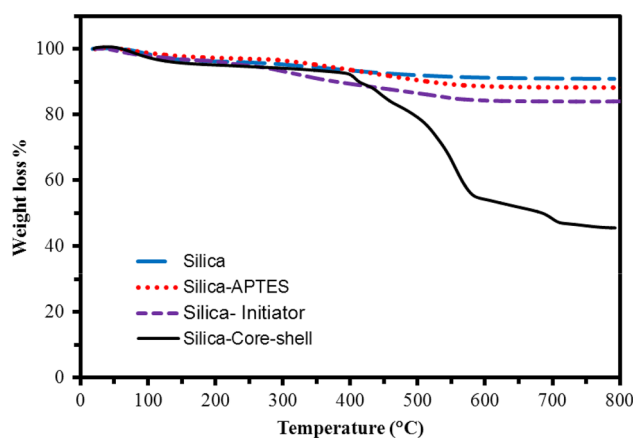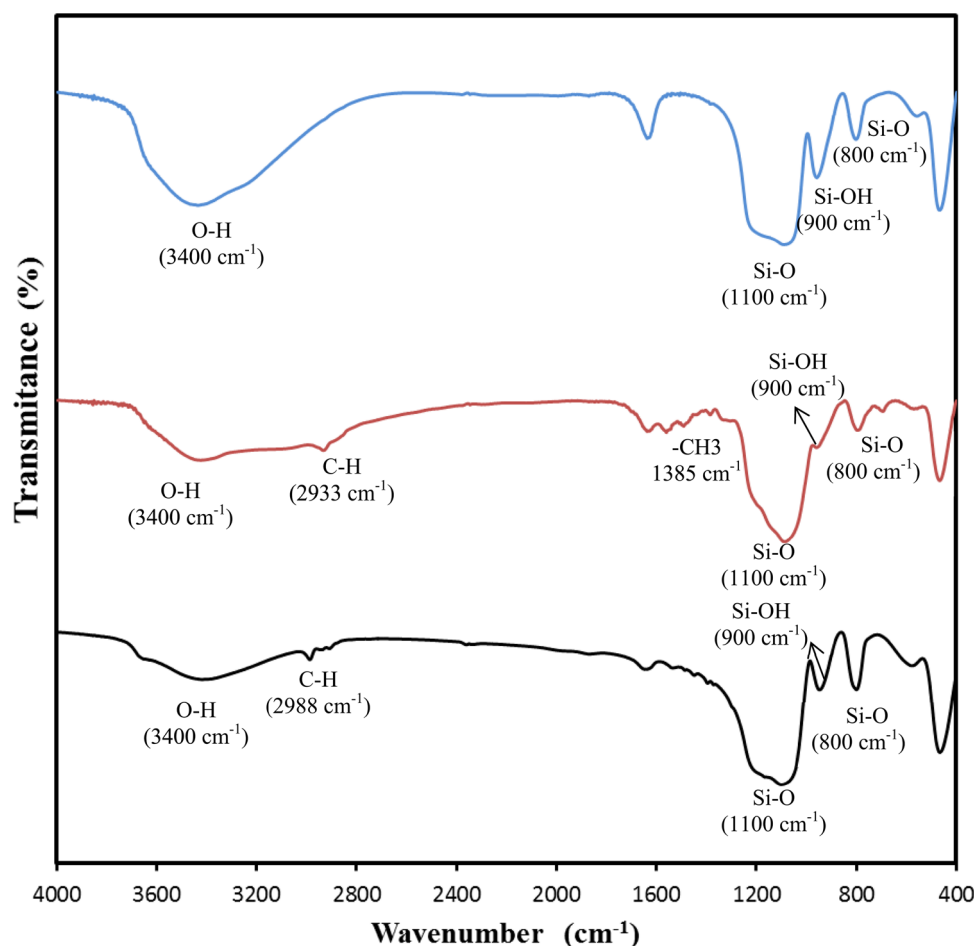
Fig. 5 Thermal gravimetric analysis (TGA) for silica after surface modification with APTES (amine group), silica modified with initiator, and core–shell silica with PNaStS as shell

range of 3200–3700 cm^{-1} can be observed in all the samples. However, the intensity of OH peak is decreased after surface modification with APTES, and initiator as a sign of reduction in number of surface OH group. The silica with APTES are recognizable bending of –CH_3 at
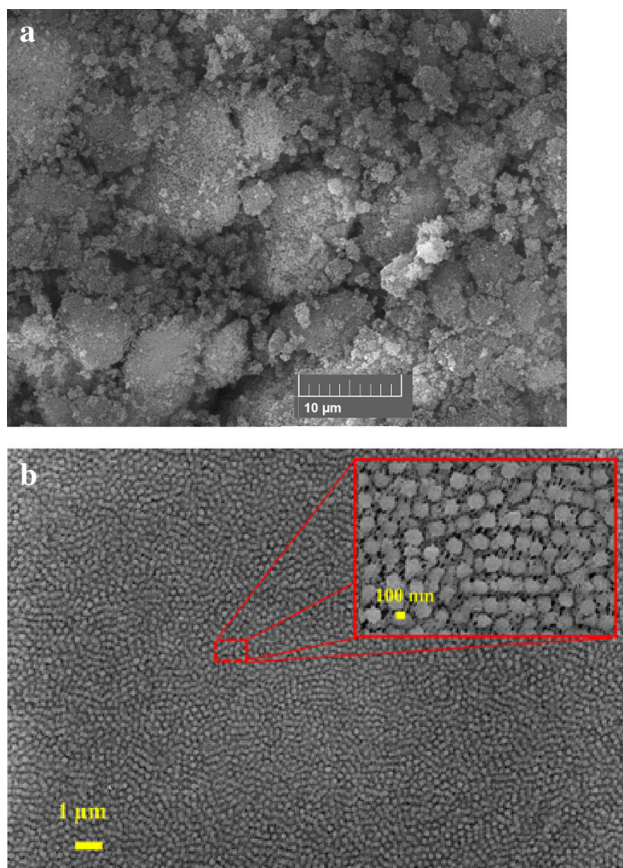
1385 cm^{-1} and stretching of C–H at 2933 cm^{-1} for alkanes. For the initiator-modified silica, the C–H peak was shifted to 2988 cm^{-1}. Because of superimposition with Si–O peak in range of 510–650 cm^{-1}, the peak for C–Br cannot be distinguished.

The weight loss of nanoparticles after modification is obtained using TGA. It can be observed in Fig. 5 that the weight loss for silica after modification with APTES, initiator, and surface-initiated polymerization is 11.8, 16, and 54% denoting an increase in organic content after each modification. As shown in Table 1, considering the surface area obtained from BET surface area measurement (96 m^2/g), carbon to hydrogen molar ratio from elemental analysis (2.9 C/H), and the number of hydroxyl group per nm^2 (5 hydroxyl group per nm^2), (Zhuravlev 1987) the grafting density of APTES on silica nanoparticles is equal to 0.83 molecule per nm^2 which is comparable with literature value of 1.2 molecule per nm^2 (Cuoq et al. 2013).

Morphology of the polymer membranes of PVDF unmodified and modified with silica nanoparticles after surface-initiated ARGET-ATRP modification with PNaStS was examined by scanning electron microscopy is shown in Fig. 6. As can be observed, porous membrane with small,

Table 1 Mole percentage and molar ratio results obtained from elemental analysis for the APTES modified silica nanoparticle

Sample	N %	C %	H %	C/N	C/H
Silica-APTES	0.65	4.06	1.39	6.22	2.90

Fig. 7 AC impedance spectroscopy for both cells at room temperature
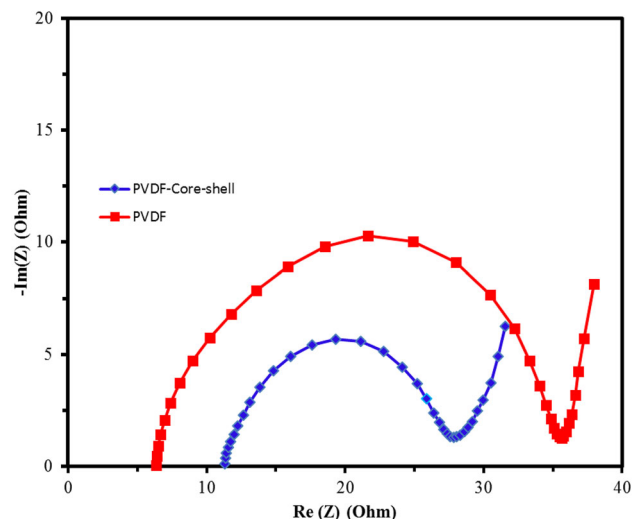
Fig. 6 Scanning electron microscopy (SEM) of electrolyte membrane **a** unmodified and modified with core–shell silica nanoparticles

pore size of 20–50 nm, and uniformly distributed pores was obtained. The porous structure was formed because of solvent/non-solvent phase separation; a structure which is necessary for both absorption of liquid electrolyte and formation of gel electrolyte and also formation of nanochannels for ion conductivity.

The AC impedance spectroscopy was performed on the Li/S-KB cell with a potentiostat (VMP3, BioLogic) over the frequency range from 0.1 Hz to 1 MHz at room temperature, and the results are shown in Fig. 7.

As it can be seen, both battery cells have a low ohmic resistance indicating easy lithium ion conduction in these cells. Interestingly, the battery cell with the PVDF-core shell particles have a lower charge transfer resistance (R_{ct}) attributed to the fast reaction kinetics within this cell. In this case, dissolution and diffusion of the generated intermediate polysulfides into the electrolyte is hindered, resulting in accumulation of these intermediate products in the cathode area and slowing the electrochemical reactions between the electrodes during cycling. The calculated value for ionic conductivity of this composite displays as high as ionic conductivity of PVDF electrolyte without core–shell nanoparticles in the room temperature and was calculated 1.10 and 0.62 mS cm^{-1}, respectively.

A cyclic voltammetry (CV) of a Li/S-KB cell with the PVDF-Core shell silica electrolyte was obtained at a scan rate of 0.1 mV s^{-1} and is shown in Fig. 8a. Two well-defined reduction peaks at 2.32 and 1.97 V are observed which could be assigned to the multistep reduction mechanism of elemental sulfur. The first reduction peak around 2.32 V is generally related to the reduction of the S_8 ring to S_8^{2-}. The second reduction peak at 1.97 V is associated with reduction of the higher polysulfide species (Li_2S_n, $4 < n < 8$) to the lower polysulfide species (Li_2S_n, $n \leq 2$). The oxidation peak around 2.5 V is associated with the oxidation of polysulfides to the neutral elemental S8 (Li et al. 2008).
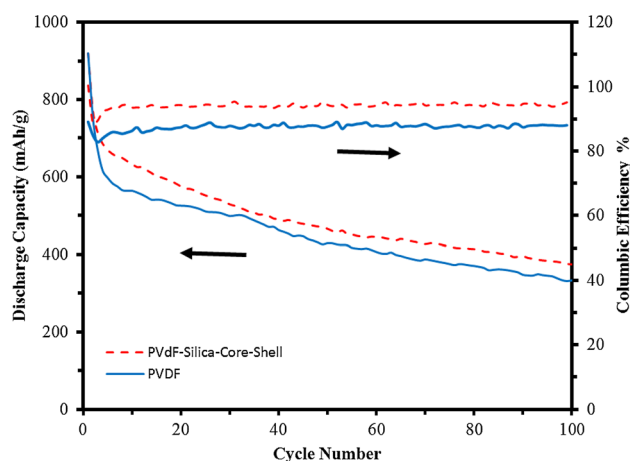
Figure 8b shows typical charge–discharge profiles for the first cycle of Li/S battery cell assembled with the composite polymer electrolyte at a constant current of 0.2 C. The series of consecutive plateaus observed in voltage profiles are those usually expected for a Li/S battery and are attributed to the electrochemical process of the cell in which a number of intermediate sulfides are involved (Kim et al. 2012). This cell delivers an initial discharge capacity of about 800 mAhg^{-1} based on the weight of sulfur active material.
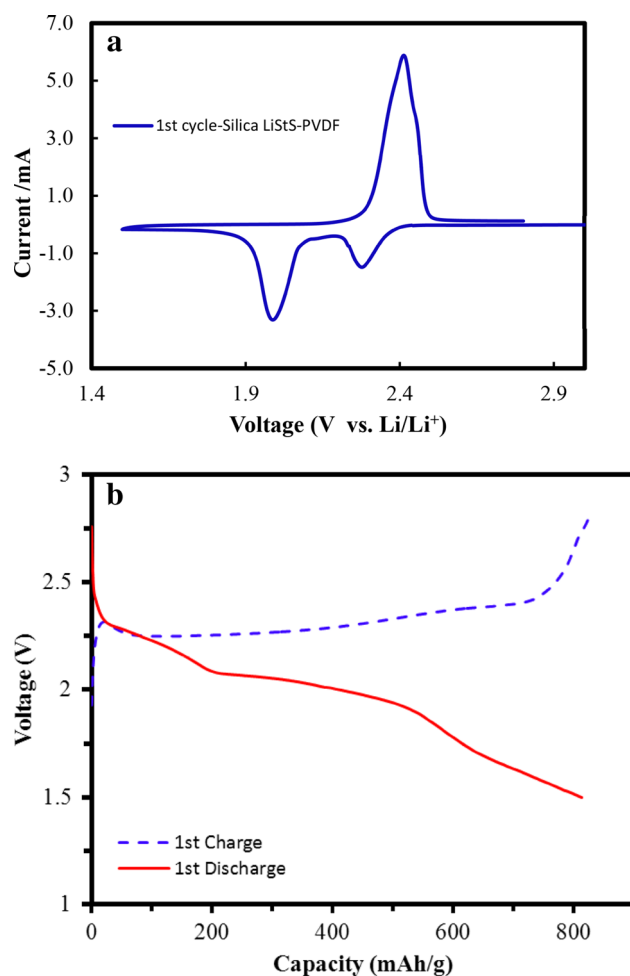
Fig. 8 Cyclic voltammetry (**a**) and charge–discharge curves (**b**) for the first cycle of sulfur/PVDF-core shell silica/lithium metal cell at scanning rate of 0.1 mV s^{-1}

Fig. 9 Discharge capacity and columbic efficiency versus cycle number at 0.2 °C rate for the sulfur/PVDF/lithium metal cell, and sulfur/PVDF-core shell silica/lithium metal cell

Conclusions

In summary, we have successfully developed a new gel polymer electrolyte (GPE) composite based on PVDF and core–shell silica nanoparticles. The surface modification on silica nanoparticles was carried out via ARGET-ATRP method using poly (vinyl benzene sulfonate) polyelectrolyte as shell. The synthesized nanoparticle was incorporated into PVDF, and then the electrochemical properties of the GPE composite with core–shell nanoparticles were studied. The role of core–shell nanoparticles was to improve cycle life of the sulfur battery through stabilization of polysulfides. The obtained GPE composite showed an ionic conductivity of 1.1 mS cm^{-1} at room temperature and better capacity retention and Columbic efficiency over hundred cycles.

References

Cuoq F, Masion A, Labille J, Rose J, Ziarelli F, Prelot B, Bottero J-Y (2013) Preparation of amino-functionalized silica in aqueous conditions. Appl Surf Sci 266:155–160. doi:10.1016/j.apsusc.2012.11.120

Das SK, Mandal SS, Bhattacharyya AJ (2011) Ionic conductivity, mechanical strength and Li-ion battery performance of mono-functional and bi-functional ("Janus") "soggy sand" electrolytes. Energy Environ Sci 4:1391–1399. doi:10.1039/C0EE00566E

Hassoun J, Scrosati B (2010) Moving to a solid-state configuration: a valid approach to making lithium-sulfur batteries viable for practical applications. Adv Mater 22:5198–5201. doi:10.1002/adma.201002584

He X, Shi Q, Zhou X, Wan C, Jiang C (2005) In situ composite of nano SiO 2–P (VDF-HFP) porous polymer electrolytes for Li-

Discharge capacity versus cycle number for both cells is shown in Fig. 9 to highlight the improvement in the performance after addition of the core–shell nanoparticles into the electrolyte membrane. Both cells exhibit almost similar initial discharge capacities. However, the Li/S cell with the composite polymer electrolyte shows better capacity retention and Columbic efficiency. For this cell, discharge capacity of 400 mAhg^{-1}, and Columbic efficiency of 95% were obtained after 100 cycles, which is consistent with literature results. _ENREF_34 (Wang et al. 2003) Such an improved Columbic efficiency indicates the excellent reproducibility of the cycles during the charge–discharge processes of the battery cell.

In charge/discharge cycle, the intermediate polysulfide spices were dissolved in gel polymer electrolyte (GPE), which reduces active sulfur during the charge–discharge process (Jin et al. 2012). For these reason the charge/discharge capacity at 100th cycle (400 mAhg^{-1}) decreased to almost half of the first cycle (800 mAhg^{-1}).

ion batteries. Electrochim Acta 51:1069–1075. doi:10.1016/j.electacta.2005.05.048

Iddon P, Robinson K, Armes S (2004) Polymerization of sodium 4-styrenesulfonate via atom transfer radical polymerization in protic media. Polymer 45:759–768. doi:10.1016/j.polymer.2003.11.030

Ji X, Lee KT, Nazar LF (2009) A highly ordered nanostructured carbon–sulphur cathode for lithium–sulphur batteries. Nat Mater 8:500–506. doi:10.1038/nmat2460

Ji L, Rao M, Zheng H, Zhang L, Li Y, Duan W, Guo J, Cairns EJ, Zhang Y (2011a) Graphene oxide as a sulfur immobilizer in high performance lithium/sulfur cells. J Am Chem Soc 133:18522–18525. doi:10.1021/ja206955k

Ji X, Evers S, Black R, Nazar LF (2011b) Stabilizing lithium–sulphur cathodes using polysulphide reservoirs. Nature communications 2:325. doi:10.1038/ncomms1293

Jin J, Wen Z, Liang X, Cui Y, Wu X (2012) Gel polymer electrolyte with ionic liquid for high performance lithium sulfur battery. Solid State Ionics 225:604–607. doi:10.1016/j.ssi.2012.03.012

Kim W-T, Jeong YU, Choi HC, Kim YJ, Song JH, Lee H, Lee YJ (2011) New anode materials of Li1 + x V1 − x O2 (0 ≤ x ≤ 0.1) for secondary lithium batteries: correlation between structures and properties. J Appl Electrochem 41:803–808. doi:10.1007/s10800-011-0299-7

Kim HS, Jeong C-S, Kim Y-T (2012) Shuttle inhibitor effect of lithium perchlorate as an electrolyte salt for lithium–sulfur batteries. J Appl Electrochem 42:75–79. doi:10.1007/s10800-011-0373-1

Kumar PR, Venkateswarlu M, Satyanarayana N (2012) Three-dimensional lithium manganese phosphate microflowers for lithium-ion battery applications. J Appl Electrochem 42:163–167. doi:10.1007/s10800-012-0383-7

Lee Y-S, Ju SH, Kim J-H, Hwang SS, Choi J-M, Sun Y-K, Kim H, Scrosati B, Kim D-W (2012) Composite gel polymer electrolytes containing core-shell structured SiO 2 (Li+) particles for lithium-ion polymer batteries. Electrochem Commun 17:18–21. doi:10.1016/j.elecom.2012.01.008

Li Z, Zhang H, Zhang P, Wu Y (2008) P (VDF-HFP)-based micro-porous composite polymer electrolyte prepared by in situ hydrolysis of titanium tetrabutoxide. J Appl Electrochem 38:109–114. doi:10.1007/s10800-007-9407-0

Li M, Yang B, Zhang Z, Wang L, Zhang Y (2013) Polymer gel electrolytes containing sulfur-based ionic liquids in lithium battery applications at room temperature. J Appl Electrochem 43:515–521. doi:10.1007/s10800-013-0535-4

Matyjaszewski K (2012) Atom transfer radical polymerization (ATRP): current status and future perspectives. Macromolecules 45:4015–4039. doi:10.1021/ma3001719

Min K, Gao H, Matyjaszewski K (2007) Use of ascorbic acid as reducing agent for synthesis of well-defined polymers by ARGET ATRP. Macromolecules 40:1789–1791. doi:10.1021/ma0702041

Mondal D, Villemure G, Song C (2014) Synthesis, characterization, and evaluation of unsupported porous NiS submicrometer spheres as a cathode material for lithium batteries. J Appl Electrochem 44:599–606. doi:10.1007/s10800-014-0658-2

Nyström D, Antoni P, Malmström E, Johansson M, Whittaker M, Hult A (2005) Highly-ordered hybrid organic-inorganic isoporous membranes from polymer modified nanoparticles. Macromol Rapid Commun 26:524–528. doi:10.1002/marc.200400617

Ohno K, Morinaga T, Koh K, Tsujii Y, Fukuda T (2005) Synthesis of monodisperse silica particles coated with well-defined, high-density polymer brushes by surface-initiated atom transfer radical polymerization. Macromolecules 38:2137–2142. doi:10.1021/ma048011q

Oriňáková R, Fedorková A, Oriňák A (2013) Effect of PPy/PEG conducting polymer film on electrochemical performance of LiFePO4 cathode material for Li-ion batteries. Chem Pap 67:860–875. doi:10.2478/s11696-013-0350-8

Reddy CVS, Chen M, Jin W, Zhu Q, Chen W, Mho S-I (2007) Characterization of (PVDF + LiFePO4) solid polymer electrolyte. J Appl Electrochem 37:637–642. doi:10.1007/s10800-007-9294-4

Ryu HS, Park JW, Park J, Ahn J-P, Kim K-W, Ahn J-H, Nam T-H, Wang G, Ahn H-J (2013) High capacity cathode materials for Li–S batteries. J Mater Chem A 1:1573–1578. doi:10.1039/C2TA00056C

Stöber W, Fink A, Bohn E (1968) Controlled growth of monodisperse silica spheres in the micron size range. J Colloid Interface Sci 26:62–69. doi:10.1016/0021-9797(68)90272-5

Thirunakaran R, Kim T, Yoon W-S (2014) Synthesis and electro-chemical characterization on dual-doped LiCoO2 via green chemistry method for lithium rechargeable batteries. J Appl Electrochem 44:709–718. doi:10.1007/s10800-014-0687-x

Ugur M, Kılıç H, Berkem M, Güngör A (2014) Synthesis by UV-curing and characterisation of polyurethane acrylate-lithium salts-based polymer electrolytes in lithium batteries. Chem Pap 68:1561–1572. doi:10.2478/s11696-014-0611-1

Wang J, Zhao Y, Zhuo K, Lin R (2002) A partial-molar volume study of electrolytes in propylene carbonate-based lithium battery electrolyte solutions at 298.15 K. Can J Chem 80:753–760. doi:10.1139/v02-092

Wang J, Liu L, Ling Z, Yang J, Wan C, Jiang C (2003) Polymer lithium cells with sulfur composites as cathode materials. Electrochim Acta 48:1861–1867. doi:10.1016/S0013-4686(03)00258-5

Wang H, Li S, Li D, Chen Z, Liu HK, Guo Z (2014) TiO_2 coated three-dimensional hierarchically ordered porous sulfur electrode for the lithium/sulfur rechargeable batteries. Energy 75:597–602. doi:10.1016/j.energy.2014.08.029

Whittingham MS (2004) Lithium batteries and cathode materials. Chem Rev 104:4271–4302. doi:10.1021/cr020731c

Yang C-M, Kim H-S, Na B-K, Kum K-S, Cho BW (2006) Gel-type polymer electrolytes with different types of ceramic fillers and lithium salts for lithium-ion polymer batteries. J Power Sources 156:574–580. doi:10.1016/j.jpowsour.2005.06.018

Yeon S-H, Jung K-N, Yoon S, Shin K-H, Jin C-S, Kim Y (2013) Improved electrochemical performances of sulfur-microporous carbon composite electrode for Li/S battery. J Appl Electrochem 43:245–252. doi:10.1007/s10800-012-0510-5

Zhan LZ, Song ZP, Zhang JY, Tang J, Zhan H, Zhou YH, Zhan CM (2008) Synthesis and properties of novel organic thiolane polymer as cathode material for rechargeable lithium batteries. J Appl Electrochem 38:1691–1694. doi:10.1007/s10800-008-9619-y

Zhang SS (2013) New insight into liquid electrolyte of rechargeable lithium/sulfur battery. Electrochim Acta 97:226–230. doi:10.1016/j.electacta.2013.02.122

Zhang P, Yang L, Li L, Ding M, Wu Y, Holze R (2011) Enhanced electrochemical and mechanical properties of P (VDF-HFP)-based composite polymer electrolytes with SiO 2 nanowires. J Membr Sci 379:80–85. doi:10.1016/j.memsci.2011.05.043

Zhang Z, Zhang Z, Wang X, Li J, Lai Y (2014) Enhanced electrochemical performance of sulfur cathode by incorporation of a thin conductive adhesion layer between the current collector and the active material layer. J Appl Electrochem 44:607–611. doi:10.1007/s10800-014-0660-8

Zhuravlev L (1987) Concentration of hydroxyl groups on the surface of amorphous silicas. Langmuir 3:316–318. doi:10.1021/la00075a004